Chlorine - hydroxyl diffusion in pargasitic amphibole

Wen Su[1], Don.R. Baker[2], Luping Pu[3], Liping Bai[2], Xin Liu[1], Cedrick O'Shaughnessy[2]

[1]State Key Laboratory of Lithospheric Evolution, Institute of Geology and Geophysics, Chinese Academy of Sciences, Beijing 100029, China;
[2]Earth and Planetary Sciences, GEOTOP-UQAM-McGill Research Centre, McGill University, 3450 rue University, Montreal, QC, Canada H3A OE8;
[3]Guilin University of Technology, Guilin 541004, China

ABSTRACT

Chlorine - hydroxyl diffusion was measured in pargasitic amphibole from Yunnan province, China at 1.0 GPa, 625 to 800 °C. Experiments were performed by immersing unoriented crystals in water-bearing NaCl in a piston cylinder for durations from 100 to 454 hours. Diffusion profiles were on the order of > 10's of micrometers in length, and electron microprobe analysis allow us to extract semi-quantitative diffusivities from these experiments. The preliminary diffusion coefficients for chlorine in amphibole in the water-bearing experiments are 2.6×10^{-16} m^2 s^{-1} at 625 °C, 4.9×10^{-16} m^2 s^{-1} at 650 °C, 7.6×10^{-16} m^2 s^{-1} at 700 °C, 1.8×10^{-15} m^2 s^{-1} at 750 °C, 2.8×10^{-15} m^2 s^{-1} at 800 °C. For temperatures between 625 and 800 °C, the Arrhenius relation for chlorine - hydroxyl diffusion has an activation energy of 106.6 ± 7.8 kJ/K mol and a D_0 of 4.53 (+7.3, -2.8) $\times 10^{-10}$ m^2 s^{-1}. Our measurements do not show evidence of anisotropy in the diffusion of Cl-OH into amphibole, but future experiments need to better investigate this possibility.

Keywords: diffusion, chlorine - hydroxyl, pargasitic amphibole, crystal-chemistry, high temperature and pressure

INTRODUCTION

Understanding the exchange of volatiles in geochemical reservoirs and recycling in Earth's interior are one of the central issues of terrestrial geodynamics (e.g. Magenheim et al., 1995; Philippot et al., 1998; Su et al., 2004; Wallace, 2005; Wood and Normand, 2008). The major volatiles in Earth's crust and upper mantle are H_2O, CO_2, S, F, and Cl (e.g. Symonds et al., 1994; Philippot et al., 1998; Wallace, 2001; Berlo et al., 2004; Self et al., 2008; Koleszar et al., 2007; Aiuppa et al., 2009; Rowe et al., 2009), but their partitioning between various phases and their mechanisms of transport in the crust and upper mantle still remain somewhat enigmatic despite decades of research. In particular, the behaviour of chlorine and fluorine at high-grade metamorphic conditions is little understood (Xiao et al., 2005; Liu et al., 2009). Knowledge of F-Cl-OH partitioning between various minerals as a function of temperature and pressure will help to constrain the Cl and F budgets of the Earth (e.g. Zhu et al., 1991; Siahcheshm et al., 2012; Rasmussen and Mortensen, 2013).

Amphiboles are important reservoirs for volatile components such as H_2O, Cl and F (e.g. Kullerud, 1996; McCormick et al., 1999) and are stable in a wide range of pressure-temperature conditions (e.g. Wones and Gilbert, 1982; Maresch et al., 2007; Ruiz Cruz, 2010). They can be used as indicators of temperature, pressure, volatile content, and oxidation state of their host rocks (e.g. Popp et al., 1995; Hawthorne et al., 1998; King et al., 1999; 2000; Evans, 2007; Oberti et al., 2007). They also provide information on the petrogenesis and thermo – mechanical evolution of rocks through

47 their structural phase transitions and crystal – chemical behavior (Boffa Ballaran et al.,
48 2004; Iezzi et al., 2006; Oberti et al., 2007; Tiepolo et al., 2007; Welch et al., 2007; Su
49 et al., 2009).

50 Cl concentrations in amphibole can be used to study the salinity of the fluid with
51 which they were last in equilibrium (e.g. Vanko, 1986; Stakes et al., 1991; Markl et al.,
52 1998a; 1998b; Philippot et al., 1998). If brine is involved in metamorphism this fluid
53 can not only affect the stability of the minerals in the rocks, but its presence should be
54 also recorded in the compositions of minerals (Philippot et al., 1995; Glassley, 2001;
55 Svensen et al., 2001; Liu et al., 2009). Therefore, the study of Cl concentrations in
56 amphiboles is particularly helpful in interpretation of the chlorinity of the fluid, and
57 the variation of Cl concentrations in amphibole possibly provides information on the
58 compositional evolution of fluids during tectonic evolution (e.g., Thompson and
59 England, 1984; Sharp and Barnes, 2004; Rowe et al., 2009; Engvik et al., 2011).

60 The rate of attainment of equilibrium concentrations of Cl in amphibole is most
61 probably controlled by Cl diffusion in many cases. However investigations of Cl
62 diffusion in amphibole are lacking (Cherniak and Dimanov, 2010; Farver, 2010),
63 although the diffusion kinetics of the hydrogen, oxygen, F-OH, Sr and Ar were
64 measured in amphiboles by Graham et al. (1984), Ingrin and Blanchard (2000, 2006),
65 Farver and Giletti (1985), Brabander et al. (1995), Brabander and Giletti (1995),
66 Harrison (1981) and Baldwin et al. (1990), respectively. In order to improve
67 knowledge of Cl diffusion in amphibole, reconnaissance experiments were performed
68 at 1.0 GPa and temperatures between 625 and 800 °C in the presence of a binary

(H_2O–NaCl) brine to measure the diffusion coefficients of chlorine in pargasitic amphiboles. Although diffusion itself cannot explain large scale transport properties, this process represents a fundamental mechanism in the modeling of chlorine behavior in amphiboles.

EXPERIMENTAL AND ANALYTICAL TECHNIQUES

Starting material

Sample JL used in this study was collected from marble of Yunnan province, China. The rock is composed of very coarse homogeneous crystals of amphibole (Fig. 1a, b), clinopyroxene, orthopyroxene, epidote, plagioclase (Fig. 1b-d, Table 1). The fine grained matrix mainly consists of calcite, dolomite (Fig. 1a, b, c) and minor quartz, biotite, titanite, apatite, zircon, magnetite, ilmenite and chromite (Fig. 1c, d, Table 1). The amphibole is emerald-green, translucent to transparent, with a vitreous luster. The individual crystals are large (from 12 to 15 × 8 to 10 mm, and sometimes as large as 36 × 14 mm) and well-formed (Fig. 1a). The amphiboles are optically pure and free of major fractures and inclusions. Table 1 lists the chemical composition of the starting amphibole. Electron microprobe analysis and back-scattered electron images show that the amphibole crystal is homogeneous in composition from core to rim (Table 1, Fig. 1e). Crystal chemical formulae were calculated on the basis of 23 oxygens with all iron considered to be ferrous. According to the classification of Leake et al. (1997), sample JL is a pargasite. These pargasitic amphiboles are characterized by higher MgO (20.4 wt %), CaO (13.5 wt %) contents, and the lower

91 FeO_T contents (0.15 wt %) (Table 1), than parasites from other geological
92 environments (e.g., Liu et al., 2009). They contain a high fluorine content with 0.34 -
93 0.38 wt% (Table 1), which is similar to that of Mg-rich amphiboles in
94 high-temperature marbles (e.g., Petersen et al., 1982; Valley et al., 1982). They also
95 contain low chlorine concentrations, ranging from 0.036 to 0.041 wt% (average 0.039
96 wt %).
97 The rock was crushed with a hammer, and the amphibole crystals hand-picked.
98 The crystals were cleaved into sub-cubic pieces by hand with an average grain size of
99 approximately 1-2 mm on edge for loading into capsules. Other portions of the
100 amphiboles were ground under alcohol in an agate mortar and pestle to powder of less
101 than 50 micrometers in size. This powder was mixed with reagent-grade NaCl in a
102 weight ratio of 2:1 (NaCl to amphibole).
103
104 **Experimental procedure**
105 Experiments on chlorine - hydroxyl diffusion of pargasitic amphibole were
106 performed at a piston cylinder at Earth and Planetary Sciences in McGill University.
107 The capsules used in the experiment are platinum tubes with a 3.0 mm outer diameter
108 that cut to 6.0-7.0 mm in length, and cleaned in concentrated hydrofluoric acid,
109 repeatedly washed with distilled water, cleaned in the ultrasonic bath, annealed to
110 orange heat, and the bottom crimped and welded. For each diffusion experiment a Pt
111 capsule was approximately half-filled with the amphibole-NaCl mixture then a
112 randomly oriented piece of amphibole crystal was loaded followed by more of the

amphibole-NaCl mixture. Water (0.23-3.81µg, Table 2) was also introduced into the capsule prior to the addition of the amphibole-NaCl mixture. The Pt capsule was welded closed without volatile loss, and put into the oven a 120 °C for 24 hours, and weighed again to check for leakage. The Pt capsule was then placed inside a graphite cylinder with a 3.0 mm inner diameter and covered with graphite lid. Two Pt capsules (one with water, another without water) were inserted into a graphite cylinder, placed into crushable alumina and surrounded by pyrophyllite powder to ensure that the water was not lost during experiments. The capsules were located in the center of a 19.1 mm crushable alumina – graphite – Pyrex – NaCl assembly (Baker, 2004). The assemblies were pressurized and heated to 1.0 GPa, and temperatures between 625 and 800 °C in a piston-cylinder apparatus. The run procedure consisted of simultaneously pressurizing and heating the assembly. A constant heating rate of 100 °C /min was used, which resulted in less than a 5 °C overshoot of the run temperature. Temperatures were measured with type C thermocouples. Pressures were controlled within ± 0.08 GPa and temperatures within ± 2 °C of desired conditions. All experimental durations (between 100 and 454 hours, Table 2) are based upon the time at which the experiment reached the desired run temperature. Samples were quenched from run temperature within 30 s by turning off the power of the piston-cylinder. After quenching, the capsules were mounted in epoxy, sectioned longitudinally and polished for electron microprobe analysis of the Cl concentrations to acquire the diffusion profiles.

Electron microprobe analysis

Electron microprobe analysis (EMPA) was first performed using the JEOL 8900 Electron Microprobe at McGill University. The accelerating voltage was 15 kV, with a beam current of 20 nA; the beam size was 1 μm in diameter. One of the main caveats associated with diffusion modeling is ensuring that the chemical profile used within the model is of sufficient spatial resolution so as to avoid complications linked with overlapping analyses and the smearing out of profiles that result in convolution effects (e.g., Ganguly et al. 1988; Costa and Morgan 2010). The effects of convolution become less severe as the diffusion profile lengthens (Ganguly et al. 1988). To minimize the convolution problem, the diffusion profiles were also measured by the JXA-8100 Electron Microprobe at the State Key Laboratory of Lithospheric Evolution, Institute of Geology and Geophysics, Chinese Academy of Sciences (IGGCAS). The diffusion profile was analyzed using a step size of 3 micrometers by sweeping the electron beam across the interface of a diffusion couple of a fixed sample stage, with a beam size of 1 μm in diameter. The standards were diopside for Si, Ca and Mg, hematite for Fe, orthoclase for Al and K, albite for Na, chromite for Cr, rutile for Ti, spessartine for Mn, fluorite for F and vanadinite for Cl. The accelerating voltage was 15 kV, with a beam current of 40 nA. A counting time of 20 s on the peak was used for all the elements except F and Cl. 40 s and 80 s counting time on the peak was used for F (LDE1) and Cl (PETH) measurements, respectively. Backgrounds were measured for half the counting times used on the peaks. Additionally, X-ray distribution maps of the Cl, Fe, Mg concentrations in the amphiboles were performed using a

Camcea SX Five Electron Microprobe. The accelerating voltage was 15 kV, with a beam current of 200 nA and dwell of 100 ms; the step size for the maps was 1 micrometers the map size was 1024 × 1024 pixels.

In order to further identify EMPA data accuracy, $^{37}Cl/^{30}Si$ profile of the amphibole was conducted using a CAMECA Nano-SIMS 50L at the State Key Laboratory of Lithospheric Evolution, IGGCAS. An amphibole transverse and depth profile consists of monitoring the intensities of ^{16}O, ^{35}Cl, ^{37}Cl, ^{30}Si, and ^{19}F signals as the primary ion beam sputters into the amphibole using the multi-collector mode. The instrument was operated with Cs^+ primary ion beam, which was accelerated at 16 keV, with an intensity of ~70 pA and a beam size of ~0.5 μm in diameter at the sample surface. The beam was scanning within an area of 1.5 μm. The mass resolution was set to 6000 (CAMECA definition) to obtain a flat top at the mass peak. There was an acquisition time of ~150 s for each analyses point, a data was obtained by 30 cycles for 15 s, and 10 sections of data in the same position.

RESULTS

Calculation of chlorine diffusion coefficients from concentration profiles

The back-scattered electron images show no evidence that the experimental amphibole crystals experience dissolution or regrowth (Fig. 2). The analytical traverses were used to calculate chlorine diffusivity. Chlorine concentrations were plotted vs. distance (Fig. 3, 4), and the diffusion coefficients were calculated for each experiment (Table 2). Diffusivities were determined from chlorine profiles using

Equation 3.13 in Crank (1975), which assumes a constant diffusivity and that the diffusion from the surface of a single crystal has not reached the center of the sample (hence a semi-infinite medium):

$$C(x,t) = (C_0 - C_1) * erf\,(x/(2*(Dt)^{0.5}) + C_1 \qquad (1)$$

where $C(x, t)$ is the chlorine concentration along the diffusion profile plotted in a concentration vs. distance diagram; x is the distance along the profile (in meters); and t is the experimental duration (in seconds); C_0 is the original concentration in the sample; C_1 is the surface concentration of the chlorine; *erf* is the error function; D is the diffusion coefficient or diffusivity (m^2s^{-1}). The error of each diffusivity measurement is estimated based upon multiple microprobe traverses on the same experiment. The run products of almost all experiments were analyzed by performing multiple microprobe traverses: 8 traverses for No. 1 (4 perpendicular to the long axis and others parallel to the long axis, respectively); 8 traverses each for No. 3, No. 5, (4 perpendicular to the long axis and others parallel to the long axis, respectively); 6 traverses for No. 7 (all perpendicular to the long axis); 6 traverses for No. 10 (3 perpendicular to the long axis and others parallel to the long axis, respectively). The step size for all of the traverses is 3 micrometers. In order to avoid the convolution effect of the surrounding NaCl, each calculation of the Cl diffusion coefficient did not use the first two points of the profile. In addition, one traverse profile of the run No. 3 of the experiment was measured by Nano-SIMS. This profile has 22 points (Fig. 4b). The beam is rastered upon the surface of the sample to produce a homogeneously sputtered flat-bottomed crater of approx 3 x 2μm area (Fig. 4a). The sputtering rate

for each analysis point in the amphibole was determined by monitoring crater depth as a function of time. Sputtering was allowed to proceed for about 150 seconds so as to define the complete diffusion profile and produce the $^{37}Cl/^{30}Si$ ratio to a depth of 0.66μm with 10 sections of data in the same position. The signal from each mass was monitored for 15 seconds to provide a statistically significant count rate by measuring 30 cycles. A computer program written in Scilab was used to compute diffusivities from each diffusion profile (Figs. 3, 4).

Diffusivity calculations for the experiments

All experiments produced extremely short diffusion profiles due to the slow diffusivity of Cl in amphibole at metamorphic conditions. Thus, we consider the results of this study to be preliminary, but nevertheless important because of the paucity of Cl diffusion measurements in amphiboles and the importance of Cl in amphibole.

The diffusivity was 2.6×10^{-16} m^2 s^{-1} (Fig. 3a, Table 2) in the experiment at 625 °C and 454 h. At 650 °C, 100 h, the diffusion coefficient for Cl in amphibole in the experiment was 4.9×10^{-16} m^2 s^{-1} (Fig. 3b, Table 2). The 700 °C, 200 h experiment yielded a diffusion coefficient of 7.6×10^{-16} m^2 s^{-1} (Fig. 3c, Table 2). At 750 °C and 200 h, the diffusion coefficients of experiment are 1.8×10^{-15} m^2 s^{-1} by EMP analysis and 1.9×10^{-15} m^2 s^{-1} by SIMS analysis (Figs. 3d and 4, Table 2). The diffusivity of Cl in the amphibole at 800 °C measured in the 100 h experiment is 2.8×10^{-15} m^2 s^{-1} (Fig. 3e, Table 2).

Although we did not orient our crystals, we used cleaved samples and performed diffusion profiles along approximately perpendicular traverses of the polished sections to search for anisotropic diffusion. Our measurements do not demonstrate any evidence of anisotropy in the diffusion on Cl into amphibole; however anisotropic effects might be smaller than our estimated uncertainty in the diffusion measurements of ± 50 relative percent.

DISCUSSION

Effect of temperature

The temperature dependency of chlorine diffusion was characterized via an Arrhenius equation (Fig. 5) at constant pressure:

$$D = D_0 \exp(-Ea / RT) \qquad (2)$$

where D is the diffusion coefficient ($m^2\ s^{-1}$), D_0 is the preexponential factor, Ea is the activation energy (kJ mol^{-1}), R is the gas constant (J K^{-1} mol^{-1}) and T the temperature (degrees Kelvin).

The Arrehenius plot describing chlorine diffusion is displayed in Figure 5. Fitting the water-bearing experiments between 625 °C and 800 °C yields an activation energy for Cl diffusion of 106.6 ± 7.8 kJ/K mol and a D_0 of 4.53 (+7.3/-2.8) × 10^{-10} m^2s^{-1} with a correlation coefficient of 0.9921 (Fig. 5). These data are for P = 1GPa.

Comparisons with the diffusion of other elements in amphibole

Very few studies have been performed on the diffusion of cations and anions in

amphiboles, although the importance of understanding metasomatic processes in such common minerals is great. Graham et al. (1984) reported the hydrogen diffusion kinetics in amphiboles for a range of compositions including hornblende, tremolite, and actinolite at 350 - 800 °C, 0.2 - 0.8 GPa confining pressure. The value of diffusion coefficients were obtained from bulk exchange with water of different hydrogen isotope composition, and yielded Arrhenius relations with activation energies of 79-84 kJ/mol for hornblende, 71.5 kJ/mol for tremolite, and 99 kJ/mol for actinolite. Ingrin and Blanchard (2000) measured the hydrogen diffusion coefficient in natural kaersutite crystals at 600 - 900 °C and 0.01 GPa pressure and found an activation energy of 104 ± 12 kJ/mol. In addition, Ingrin and Blanchard's (2000, 2006) data clearly demonstrate that hydrogen diffusion in amphibole is anisotropic: transport along the *c*-axis faster than along the *b*-axis. The only experimental data on oxygen diffusion in amphiboles was reported by Farver and Giletti (1985); they measured oxygen diffusivity in a range of amphibole compositions including hornblende, tremolite, and fluor-richterite at 650 - 800 °C at 0.1 GPa pressure, and determined activation energies of 172 ± 25 kJ/mol for hornblende, 163 ± 21 kJ/mol for tremolite, and 238 ± 8 kJ/mol for fluor-richterite. Brabander et al (1995) measured F-OH interdiffusion in tremolite over the temperature range 500 - 800 °C and 0.2 GPa pressure and obtained an activation energy of 41 ± 5 kJ/mol and a pre-exponential factor of 3.4×10^{-17} $m^2 s^{-1}$. Measurements of Ar diffusion in amphibole were reported by Harrison (1981) and Baldwin et al. (1990).

Figure 6 summarizes all published diffusion data for amphibole and the

comparison to our results. Our measured Cl diffusivities lie between those obtained for hydrogen isotopic exchange (Graham et al., 1984), F-OH interdiffusion (Brabander et al. 1995) and oxygen isotopic exchange (Farver and Giletti, 1985). The measured activation energy in this study of Cl is similar to that of H diffusion, but significantly higher than F-OH diffusion (Fig. 6).

It is well known that both ionic charge and radius affect diffusion in crystals (Van Orman et al., 2001; Tirone et al., 2005; Carlson et al., 2012). When ions have the same charge and reside in the similar crystalline sites it is expected that the smaller ion would display a higher diffusivity than the larger ion (Zhang et al., 2006, 2010). Oberti et al. (1993) found that F and OH, with radii of 0.130 nm and 0.135 nm, respectively (Hawthorne and Oberti, 2007), are found in the O(3) amphibole site, but that larger Cl, with a 0.181 nm radius (Shannon, 1976), is found in a slightly displaced position, the O(3)' site. Because of the same charge and the occupancy of similar sites in amphibole, Cl is expected to diffuse more slowly than F, opposite to the comparison of Brabander et al.'s results (1995) and this study.

The anomalous behavior of Cl in comparison to F is reflected in its high pre-exponential factor in the Arrhenius equation. The pre-exponential factor is classically associated with the square of the distance between two stable sites multiplied by a vibrational frequency of the atom (see Eqn. 158 in Glasstone et al., 1941). We speculate that the small differences in the location of the sites for Cl and F in the amphibole structure are significant enough to affect the pre-exponential factor through modification of the distance between two stable sites and the vibrational

frequency of the Cl. However, we have no further evidence to support this speculation and perhaps the differences in the experimental procedures (e.g., pressure, chemical potential gradients) and amphibole compositions between our study and that of Brabander et al. (1995) might play a significant role in explaining the surprising measurements of F and Cl diffusion in amphibole.

Effect of Cl on the amphibole chemistry and structure

The *M*(1) and *M*(3) sites of amphibole are coordinated by the O(3) or O(3)' site, which contains (OH), F^- and Cl^- or O^{2-} These are the only anion sites in the amphibole structure (e.g. Leake, 1968; Leake et al., 1997; Leake et al., 2003; Hawthorne and Oberti, 2007). The bond-valence of the <M(3)-O(3) > varies in different amphibole structures, such that the <M(3)-O(3)> distance is 0.382 A°, 0.367 A°, 0.361 A° , 0.300 A° for pargasite, cummingtonite, tremolite, and fluororichterite, respectively (Hawthorne and Oberti, 2007). Comodi et al. (1991) found that the sequence of isothermal polyhedral bulk moduli are *KM*(3) > *KM*(1) > *KM*(4)> *KM*(2) in their study of tremolite, pargasite and glaucophane to 4.0 GPa. It is obvious that *M*(3) and *M*(1) are more controlled by pressure, as Zhu et al. (1991) suggested the Cl^- contents of fluids depend strongly on pressure when temperature is below 500°C. Variation of the *M*(1) and *M*(3) site volumes can lead to variations in <*M*(1)-O(3)> and <*M*(3)-O(3)> distances and variable occupancy of OH, F, Cl and O in the different amphiboles. Cl is negatively correlated with F in the amphiboles (Fig. 7a): Cl concentrations increase with decreasing F concentrations. This behavior implies that

the incorporation of Cl in amphibole may result in replacement of F at O(3) in the amphibole structure. Cl and F are coupled in the amphiboles studied (Figs. 2, 7b-e): Cl concentrations increase with increasing FeO and decreasing MgO (Figs. 7b and c), whereas F concentrations demonstrate the opposite behavior (Figs. 7d, e). However, how the diffusion coefficients of Fe and Mg in the amphibole compare to Cl is currently not clear. Therefore, further research on correlations between (Cl, F, OH) occupancy on the hydroxyl site and (Mg, Fe) occupancy on the octahedral site during Cl replacement with F or OH at high temperature and pressure are needed.

IMPLICATIONS

Diffusion of chlorine in amphibole is an important area of study, with applications in improving understanding of volatile transport, so the first chlorine diffusion results of the pargasitic amphibole have value. Although Cl diffusion itself cannot explain large- or micro- scale transport properties, this process represents a fundamental mechanism controlling Cl behavior during crystallization, assimilation and metamorphism. Compositionally zoned minerals, combined with kinetic modeling of chemical gradients, can be used to provide a chronological tool that can access a large range of time scales and can be applied to rocks of any age (e.g., Zellmer et al., 1999; Coombs et al., 2000; Klügel, 2001; Pan and Batiza, 2002; Morgan et al., 2004; Costa and Chakraborty, 2008), if the processes responsible for zoning and the relevant diffusivities are available. Broader implications and applications of our study are that modeling the Cl chemical gradients in amphiboles

and combining these results with modeling of other cations can provide a unique window into the time scales of metamorphic/metasomatic process, which is impossible to achieve by any isotopic method, because often the durations of events, particularly retrograde metamorphic events, may be too short to measure isotopically.

ACKNOWLEDGMENTS

This study was funded by the NNSFC (No. 41172066 and 41021063), the State Key Laboratory of Superhard Materials, and a Canadian Discovery Grant. We greatly appreciate Mr. Tianwen Lan for very generously donated the amphibole-bearing marble samples, Prof. Jingbo Liu for the amphibole profile of the eclogite from the Yangkou, China, Dr. Lang Shi, Dr. Qian Mao and Jianchao Zhang for microprobe and Nano-SIMS measurements. We also thank Dr. Youxue Zhang for critical and constructive comments. The paper benefited considerably from the critical reviews of Drs F. Costa, D.J. Cherniak and H. Sato.

REFERENCES CITED

Aiuppa, A., Webster, J.D., and Baker, D.R. (2009) Halogens in volcanic systems. Chemical Geology, 263, 1-18.

Baker, D.R. (1990) Chemical interdiffusion of dacite and rhyolite: anhydrous measurements at 1 atm and 10 kbar, application of transition state theory, and diffusion in zoned magma chambers. Contributions to Mineralogy and Petrology, 104, 407-423.

Baker, D.R. (2004) Piston-cylinder calibration at 400 to 500 MPa: a comparison of using water solubility in albite melt and NaCl melting. American Mineralogist, 89, 1553-1556.

Baldwin, S.L., Harrison, T.M., and Fitz Gerald, J.D. (1990) Diffusion of ^{40}Ar in metamorphic hornblende. Contributions to Mineralogy and Petrology, 105, 691-703.

Beard, J.S. and Day, H.W. (1986) Origin of gabbro pegmatite in the Smartville intrusive complex, northern Sierra Nevada, California. American Mineralogist, 71, 1085-1099.

Berlo, K., Blundy, J., Turner, S., Cashman, K., Hawkesworth, C., and Black, S. (2004) Geochemical precursors to volcanic activity at Mount St. Helens, USA, Science, 306, 1167-1169.

Boffa Ballaran, T., Carpenter, M.A., and Domeneghetti, M.C. (2004) Order-parameter variation through the $P2_1/m \leftrightarrow C2/m$ phase transition in cummingtonite. American Mineralogist, 89, 1717-1727.

Brabander, D.J., Hervig, R.L., and Jenkins, D.M. (1995) Experimental determination of F-OH interdiffusion in tremolite and significance to fluorine-zoned amphiboles. Geochimica et Cosmochimica Acta, 59, 3549-3560.

Candela, A., and Holland, D. (1984) The partitioning of copper and molybdenum between silicate melts and aqueous fluids. Geochimica et Cosmochimica Acta, 4, 373-380.

Carlson W.D. (2012) Rates and mechanism of Y, REE, and Cr diffusion in garnet.

American Mineralogist, 97, 1598-1618.

Castelli, D. (1998) Chlorpotassium ferro-pargasite from Sesia-Lanzo Marbles (Western Italian Alps): a record of highly saline fluids. Rend SIMP, 43, 129-38.

Cherniak, D.J. (2010) Cation diffusion in feldspars. Reviews in Mineralogy and Geochemistry, 72, 691-734.

Chew, D.J., Sylvester, P.J., and Tubrett, M.N. (2011) U–Pb and Th–Pb dating of apatite by LA–ICPMS. Chemical Geology, 280, 200-216.

Chukanov, N.V., Konilov, A.N., Zadov, A.E., Belakovsky, D.I., and Pekov, I.V. (2002) The new amphibole potassic chloropargasite (K,Na) Ca_2 $(Mg,Fe^{2+})_4Al$ $(Si_6Al_2O_{22})$ $(Cl, OH)_2$ and conditions of its formation in the granulite complex of Salnye Tundry Massif (Kola Peninsula). Zapiski, VMO, 131, 58-62.

Coombs, M.L., Eichelberger, J.E., and Rutherford, M.J. (2000) Magma mixing and storage conditions for the 1953-1974 eruptions of Southwest trident volcano, katmai National ark, Alaska. Contributions to Mineralogy and Petrology, 140, 99-118.

Costa, F., and Chakraborty, S. (2008) The effect of water on Si and O diffusion rates in olivine and implications for transport properties and processes in the upper mantle. Physics of the Earth and Planetary Interiors, 166, 11-29.

Costa, F., and Morgan, D. (2010) Time constraints from chemical equilibration in magmatic crystals. In A. Dosseto, S.P. Turner, and J.A. Van-Orman, Eds., Timescales of Magmatic Processes: From Core to Atmosphere, Wiley-Blackwell, New York, p. 126-159.

399 Crank, J. (1975) Mathematics of Diffusion, 2nd ed. Oxford University, London Press.
400 Davis, D.W., Krogh, T.E., and Williams, I.S. (2003) Historical Development of Zircon
401 Geochronology. Reviews in Mineralogy and Geochemistry, 53, 145-181.
402 Deer, W.A., Howie, R.A., and Zussman, J. (1997) Rock Forming Minerals, Volume
403 2B, Second Edition, Double-chain Silicates. The Geological Society, London.
404 Dick, L.A., and Robinson, G.W. (1979) Chlorine-bearing potassian hastingsite from a
405 sphalerite skarn in the southern Yukon. Canadian Mineralogist, 17, 25-26.
406 Enami, M., Liou, J.G., and Bird, D.K. (1992) Cl-bearing amphibole in the Salton Sea
407 geothermal system, California. Canadian Mineralogist, 30, 1077-1092.
408 Engvik, A. K., Mezger, K., Wortelkamp, S., Bast, R., Corfu, F., Korneliussen, A.,
409 Ihlen, P., Bingen, and Austrheim, H. (2011) Metasomatism of gabbro; mineral
410 replacement and element mobilization during the Sveconorwegian metamorphic
411 event. Journal of Metamorphic Geology, 29, 399-423.
412 Evans, B.W. (2007) The Synthesis and Stability of Some End-Member Amphiboles.
413 Reviews in Mineralogy and Geochemistry, 67, 261-286.
414 Evans, B.W., and Guggenheim, S. (1988) Talc, pyrophyllite, and related minerals.
415 Reviews in Mineralogy and Geochemistry, 19, 225-294.
416 Farver, J.R. (2010) Oxygen and hydrogen diffusion in minerals. Reviews in
417 Mineralogy and Geochemistry, 72, 447-507.
418 Farver, J. R., and Giletti, B. J. (1985) Oxygen diffusion in amphiboles. Geochimica et
419 Cosmochimica Acta, 49, 1403-1411.
420 Fortier, S.M., and Giletti, B.J. (1991) Volume self-diffusion of oxygen in biotite,

muscovite, and phlogopite micas. Geochimica et Cosmochimica Acta, 55, 1319-1330.

Ganguly, J., Bhattacharya, R.N., Chakraborty, S. (1988) Convolution effect in the determination of compositional profiles and diffusion coefficients by microprobe step scans. American Mineralogist, 73, 901-909.

Giletti, B.J., Semet, M.P., and Yund, R.A. (1978) Studies in diffusion-III. Oxygen in feldspars: An ion microprobe determination. Geochimica et Cosmochimica Acta, 42, 45-57.

Glassley, W.E. (2001) Elemental composition of concentrated brines in subduction zones and the deep continental crust. Precambrian Research, 105, 371-383.

Glasstone, S., Laidler, K.J., and Eyring, H. (1941) The Theory of Rate Processes. McGraw-Hill, New York, 611 p.

Graham, C. M., Harmon, R. S., and Sheppard, S. M. F. (1984) Experimental hydrogen isotope studies: Hydrogen isotope exchange between amphibole and water. American Mineralogist, 69, 128-138.

Gulyaeva, T.Y., Gorelikova, N.V., and Karabtsov, A.A. (1986) High potassium-chlorine-bearing hastingsites in skarns from Primorye, far east USSR. Mineralogical Magazine, 50, 724-728.

Harrison, T. M. (1981) Diffusion of ^{40}Ar in hornblende. Contributions to Mineralogy and Petrology, 78, 324-331.

Hawthorne, F.C., Oberti, R., Zanetti, A., and Czamanske, G.K. (1998) The role of Ti in hydrogen-defi cient amphiboles: Sodic-calcic and sodic amphiboles from

Coyote Peak, California. Canadian Mineralogist, 36, 1253-1265.

Hawthorne, F.C., and Oberti, R. (2007a) Amphiboles: crystal chemistry. Reviews in Mineralogy and Geochemistry, 67, 1-54.

Hawthorne, F.C., and Oberti, R. (2007b) Classification of the Amphiboles. Reviews in Mineralogy and Geochemistry, 67, 55-88.

Hedenquist, J.W., and Lowenstern, J.B. (1994) The role of magmas in the formation of hydrothermal ore deposits. Nature, 370, 519-527.

Heinrich, C.A. (2005) The physical and chemical evolution of low to medium-salinity magmatic fluids at the porphyry to epithermal transition: a thermodynamic study. Mineralium Deposita, 39, 864-889.

Helgeson, H.C. (1969) Thermodynamics of hydrothermal systems at elevated temperatures and pressures. American Journal of Science, 267, 729-804.

Helgeson, H.C. (1964) Complexing and Hydrothermal Ore Deposition. MacMillan, New York, pp 128.

Iezzi. G., Liu, Z., and Della Ventura, G. (2006). Synchrotron infrared spectroscopy of synthetic Na(NaMg)Mg5Si8O22(OH)2 up to 30 GPa: Insight on a new high-pressure amphibole polymorph. American Mineralogist, 91, 479-482.

Ingrin, J., and Blanchard, M. (2000) Hydrogen mobility in single crystal kaersutite. EMPG VIII, Journal of Conference Abstracts, 5, 52.

Ingrin, J., and Blanchard, M. (2006) Diffusion of hydrogen in minerals. Reviews in Mineralogy and Geochemistry, 62, 291-320.

Ito, E., and Anderson, A.T. (1983) Submarine metamorphism of gabbros from the Mid-Cayman Rise: petrographic and mineralogic constraints on hydrothermal process at slow-spreading ridges. Contributions to Mineralogy and Petrology, 82, 371-388.

Kamenetsky, V.S., Wolfe, R.C., Eggins, S.M., Mernagh, T.P., and Bastrakov, E. (1999) Volatile exsolution at the Dinkidi Cu–Au porphyry deposit, Philippines: a melt-inclusion record of the ore-forming process. Geology, 27, 691-694.

Kamineni, D.C. (1986) A petrochemical study of calcic amphiboles from the East Bull Lake anorthosite-gabbro layered complex, District of Algoma, Ontario. Contributions to Mineralogy and Petrology, 93, 471-481.

King, P.L., Hervig, R.L., Holloway, J.R., Delaney, J.S., and Dyar, M.D. (2000) Partitioning of Fe^{3+}/Fe^{total} between amphibole and basanitic melt as a function of oxygen fugacity. Earth and Planetary Science Letters, 178, 97-112.

King, P.L., Hervig, R.L., Holloway, J.R., Vennemann, T.W., and Righter, K. (1999) Oxy-substitution and dehydrogenation in mantle-derived amphiboles megacrysts. Geochimica et Cosmochimica Acta, 62, 3635-3651.

Klügel, A. (2001) Prolonged reactions between harzburgite xenoliths and silica-undersaturated melt: implications for dissolution and Fe-Mg interdiffusion rates of orthopyroxene. Contributions to Mineralogy and Petrology, 141, 1-14.

Koleszar, A. M., Kent, A. J., Wallace, P. J., and Woodhead J. D. (2007) Volatile (H, C, Cl, S) concentrations in ocean island basalt glasses from Pitcairn and the Society Islands, Eos, 88 (Suppl.).

Kullerud, K. (1996) Chlorine-rich amphiboles: interplay between amphibole compositions and an evolving fluid. European Journal of Mineralogy, 8, 355-370.

Kullerud, K., and Erambert, M. (1999) Cl-scapolite, Cl-amphibole, and plagioclase equilibria in ductile shear zones at Nusfjord, Lofoten, Norway; implications for fluid compositional evolution during fluid–mineral interaction in the deep crust. Geochimica et Cosmochimica Acta, 63, 3829-3844.

Kullerud, K., Flaat, K., and Davidsen, B. (2001) High-pressure fluid–rock reactions involving Cl-bearing fluids in lower-crustal ductile shear zones of the Flakstadoy Basic Complex, Lofoten, Norway. Journal of Petrology, 42, 1349-1372.

Leake, B.E. (1968) A catalog of analyzed calciferous and subcalciferous amphiboles together with their nomenclature and associated minerals. Geological Society of America, Spec. Pap. 98.

Leake, B.E., Woolley, A.R., Arps, C.E.S., Birch, W.D., Gilbert, M.C., Grice, J.D., Hawthorne, F.C., Kato, A., Kisch, H.J., Krivovichev, V.G., Linthout, K., Laird, J., Mandarino, J.A., Maresch, W.V., Nickel, E.H., Rock, N.M.S., Schumacher, J.C., Smith, D.C., Stephenson, N.C.N., Ungaretti, L., Whittaker, E.J.W., and Guo, Y. (1997) Nomenclature of amphiboles: Report of the subcommittee on amphiboles of the International Mineralogical Association, Commission on New Minerals and Mineral Names. Canadian Mineralogist, 35, 219-246.

Leake, B.E., Woolley, A.R., Birch, W.D., Burke, E.A.J., Ferraris, G., Grice, J.D.,

Hawthorne, F.C., Kisch, H.J., Krivovichev, V.G., Schumacher, J.C., Stephenson, N.C.N., and Whittaker, E.J.W. (2003) Nomenclature of amphiboles: additions and revisions to the International Mineralogical Association's amphibole nomenclature. Canadian Mineralogist, 41, 1355-1370.

Li, Q.L., Lin, W., Su, W., Li, X.H., Shi, Y.H., Liu, Y., and Tang, G.Q. (2011) SIMS U–Pb rutile age of low-temperature eclogites from southwestern Chinese Tianshan, NW China. Lithos, 122, 76-86.

Liu, J.B., Liu, W.Y., Ye K., and Mao, Q. (2009) Chlorine-rich amphibole in Yangkou eclogite, Sulu ultrahigh-pressure metamorphic terrane, China, European Journal of Mineralogy, 21, 1265-1285.

Magenheim, A.J., Spivack, A.J., Michael, P.J., and Gieskes, J.M. (1995) Chlorine stable isotope composition of the oceanic crust: implications for the Earth's distribution of chlorine. Earth and Planetary Science Letters, 131, 427-432.

Maresch, W.V. and Czank, M. (2007) The Significance of the Reaction Path in Synthesizing Single-Phase Amphibole of Defined Composition. Reviews in Mineralogy and Geochemistry, 67, 287-322.

Markl, G., and Bucher, K. (1998a). Metamorphic salt in granulites: implications for the presence and composition of fluid in the lower crust. Nature, 391, 781-783.

Markl, G., and Piazolo, S. (1998b) Halogen-bearing minerals in syenites and high-grade marbles of Dronning Maud Land, Antarctica: monitors of fluid compositional changes during late-magmatic fluid–rock interaction processes. Contributions to Mineralogy and Petrology, 132, 246-268.

Matsubara, S., and Motoyoshi, Y. (1985) Potassium pargasite from Einstodingen Lutzow-Holm Bay, east Antarctica. Mineralogical Magazine, 49, 703-707.

Mazdab, F.K. (2003) The diversity and occurrence of potassium-dominant amphiboles. Canadian Mineralogist, 41, 1329-1344.

McCormick, K.A., and McDonald, A.M. (1999) Chlorine-bearing amphiboles from the Fraser mine, Sudbury, Ontario, Canada: Description and crystal chemistry. Canadian Mineralogist, 37, 1383-1403.

Meyer, C., and Hemley, J.J. (1967) Wall rock alteration. In: Barnes HL (ed) Geochemistry of hydrothermal ore deposits, 1st ed. Holt, Rinehart and Winston, New York. pp. 166-235.

Morgan, D., A. der ven, Van., and Ceder, G. (2004) Li conductivity in LixMPO4 (M = Mn, Fe, Co, Ni) olivine materials, Electrochem. Solid State Letters, 7, A30-A32.

Morrison, J. (1991) Compositional constraints on the incorporation of Cl into amphiboles. American Mineralogist, 76, 1920-1930.

Munoz, J.L. (1984) F-OH and Cl-OH exchange in micas with applications to Hydrothermal Ore Deposits. In Micas (ed. S.W. Bailey); Reviews in Mineralogy 13, pp. 469-493.

Oberti, R., Ungaretti, L., Cannillo, E., and Hawthorne, F. (1993) The mechanism of Cl incorporation in amphibole. American Mineralogist, 78, 746-752.

Oberti, R., Della Ventura, G., and Camara, F. (2007) New amphibole compositions: natural and synthetic. Reviews in Mineralogy and Geochemistry, 67, 89-123.

Pan, Y., and Fleet, M.E. (1992) Mineralogy and genesis of calc-silicates associated

552 with Archean volcanogenic massive sulphide deposits at the manitouwadge
553 mining camp, Ontario. Canadian Journal of Earth Sciences, 29, 1375-1388.
554 Pan, Y., and Batiza, R. (2002) Mid-ocean ridge magma chamber processes:
555 Constraints from olivine zonation in lavas from the East Pacific Rise at $9^0$30'N
556 and $10^0$30'N. Journal of Geophysical Research, 107, 1-13.
557 Parry, W.T., and Jacobs, D.C. (1975) Fluorine and chlorine in biotite from Basin and
558 Range plutons. Economic Geology, 70, 554-558.
559 Pekov, I.V., Chukanov, N.V., Nefedova, M.E., Pushcharovsky, D.Yu., and
560 Rastsvetaeva, R.K. (2005) Chloro-potassichastingsite (K,Na) $Ca_2(Fe^{2+},Mg)_4$
561 $Fe^{3+}[Si_6Al_2O_{22}](Cl,OH)_2$: revalidation and the new name of dashkesanite.
562 Zapiski. VMO. 134, 31-36 (Russian with English abstract).
563 Peterson, E. U., Essene, E. J., Peacor, D. R., and Valley, J. W. (1982) Fluorine end
564 member micas and amphiboles. American Mineralogist, 67, 538-544.
565 Philippot, P., Chevallier, P., Chopin, C., and Dubessy, J. (1995) Fluid composition and
566 evolution in coesite-bearing rocks (Dora-Maira massif, western Alps):
567 implication for element recycling during subduction. Contributions to
568 Mineralogy and Petrology, 121, 29-44.
569 Philippot, P., Agrinier, P., and Scambelluri, M. (1998) Chlorine cycling during
570 subduction of altered oceanic crust, Earth and Planetary Science Letters, 161,
571 33-44.
572 Philippot, P., Chevallier, P., Chopin, C., and Dubessy, J. (1995) Fluid composition and
573 evolution in coesite-bearing rocks (Dora-Maira massif, western Alps):

implication for element recycling during subduction. Contributions to Mineralogy and Petrology, 121, 29-44.

Popp, R.K., Virgo, D., and Phillips, M.W. (1995) H deficiency in kaersutitic amphiboles: experimental verification. American Mineralogist, 80, 1347-1350.

Rasmussen, K.L., and Mortensen, J.K. (2013) Magmatic petrogenesis and the evolution of (F:Cl:OH) fluid composition in barren and tungsten skarn-associated plutons using apatite and biotite compositions: Case studies from the northern Canadian Cordillera. Ore Geology Reviews, 50, 118-142.

Rowe, M.C., and Lassiter, J.C. (2009) Chlorine enrichment in central Rio Grande Rift basaltic melt inclusions: Evidence for subduction modification of the lithospheric mantle, Geology, 37, 439-442.

Rubatto, D., Gebauer, G., and Compagnoni, R. (1999) Dating of eclogite-facies zircons: the age of Alpine metamorphism in the Sesia-Lanzo Zone (Western Alps). Earth and Planetary Science Letter, 167, 141-158.

Ruiz Cruz, M. D. (2010) Zoned Ca-amphibole as a new marker of the Alpine metamorphic evolution of phyllites from the Jubrique unit, Alpujárride Complex, Betic Cordillera, Spain, Mineralogical Magazine, 74, 773-796.

Sato, H., Yamaguchi, Y., and Makino, K. (1997) Cl incorporation into successively zoned ampiboles from the Ramnes cauldron, Norway. American Mineralogist, 82, 316-324.

Sato, H., Holtz, F., Behrens, H., Botcharnikov, R., and Nakada, S. (2005). Experimental Petrology of the 1991–1995 Unzen Dacite, Japan. Part II: Cl/OH

596 Partitioning between Hornblende and Melt and its Implications for the Origin of
597 Oscillatory Zoning of Hornblende Phenocrysts. Journal of Petrology, 46,
598 197-212.

599 Self, S., Blake, S., Sharma, K., Mike, W., and Sephton, S. (2008) Sulfur and chlorine
600 in Late Cretaceous Deccan magmas and eruptive gas release. Science, 319,
601 1654-1657.

602 Shannon, R.D. (1976) Revised effective ionic radii and systematic studies of
603 interatomic distances in halides and chalcogenides. Acta Crystallographica, A32,
604 751B767.

605 Sharp, Z.D., and Barnes, J.D. (2004) Water-soluble chlorides in massive sea-floor
606 serpentinites: a source of chloride in subduction zones. Earth and Planetary
607 Science Letters, 226, 243-254.

608 Siahcheshm, K., Calagaria, A.A., Abedini, A., and Lentz D.R. (2012) Halogen
609 signatures of biotites from the Maher-Abad porphyry copper deposit, Iran:
610 characterization of volatiles in syn- to post-magmatic hydrothermal fluids.
611 International Geology Review 54, 1353-1368.

612 Sisson, V. B. (1987) Halogen chemistry as indicator of metamorphic fluid interaction
613 with the Ponder Pluton, Coast Plutonic Complex, British Columbia, Canada.
614 Contributions to Mineralogy and Petrology, 95, 123-131.

615 Sotnikov, V. I., Berzina, A. N., and Berzina, A. P. (2006) The role of metasomatism of
616 enclosing rocks in the balance of chlorine and fluorine during the ore formation

at porphyry Cu-Mo deposits. Russian Geology and Geophysics, 47, 945-955.

Stakes, D., Mevel, C., Cannat, M., and Chaput, T. (1991) Metamorphic stratigraphy of Hole 735B, in: R.P. Von Herzen, P.T. Robinson et al. (Eds.), Proc. ODP, Sci. Results 118, College Station, TX, pp. 153-180.

Su, W., Zhang, M., Redfern, S. A. T., Gao, J., and Klemd, R. (2009) OH in zoned amphiboles of eclogite from the western Tianshan, NW-China, International Journal of Earth Sciences, 98, 1299-1309.

Su,W., Ji, Z.P., Ye. K., You, Z.D., Liu J., Yu, J., and Cong, B. (2004) Distribution of hydrous components in jadeite of the Dabie Mountains. Earth and Planetary Science Letters, 222, 85-100.

Su, W., Gao, J., Klemd, R., Li, J.L., Zhang, X., Li, X.H., Chen, N.S., and Zhang, L. (2010) U–Pb zircon geochronology of Tianshan eclogites in NW China: implication for the collision between the Yili and Tarim blocks of the southwestern Altaids. European Journal of Mineralogy, 22, 473-478.

Svensen, H., Jamteit, B., Banks, D.A., and Austrheim, H. (2001) Halogen contents of eclogite facies fluid inclusions and minerals: Caledonides, western Norway. Journal of Metamorphic Geology, 19, 165-178.

Symonds, R.B., Rose, W.I., Bluth, G.J.S., and Gerlach, T.M. (1994) Volcanic-gas studies: methods, results and applications. In: Carroll, M.R., Holloway, J.R. (Eds.), Volatiles in Magmas. Reviews in Mineralogy and Geochemistry, 30, 1-60.

Thompson, A.B., and England, P.C. (1984) Pressure temperature time paths of

regional metamorphism: 2. Their inference and interpretation using mineral assemblages in metamorphic rocks. Journal of Petrology, 25, 929-955.

Tiepolo, M., Oberti, R., Zanetti, A., Vannucci, R., and Foley, S.F. (2007) Trace-element partitioning between amphibole and silicate melt. Reviews in Mineralogy and Geochemistry, 67, 417-451.

Tirone, M., Ganguly, J., Dohmen, R., Langenhorst, F., Hervig, R., and Becker, H.-W. (2005) Rare earth diffusion kinetics in garnet: Experimental studies and applications. Geochimica et Cosmochimica Acta, 69, 2385-2398.

Trommsdorff, V., Skippen, G., and Ulmer, P. (1985) Halite and sylvite as solid inclusions in high-grade metamorphic rocks. Contributions to Mineralogy and Petrology, 89, 24-29.

Tumiati, S., Godard, G., Martin, S., Kloetzli, U., and Monticelli D. (2007) Fluid-controlled crustal metasomatism within a high-pressure subducted melange (Mt. Hochwart, Eastern Italian Alps) (in Melting, metasomatism and metamorphic evolution in the lithospheric mantle). Lithos, 94, 148-167.

Valley, J.W., Petersen, E.U., Essene, E.J., and Bowman, J.R. (1982) Fluorphlogopite and fluortremohte in Adirondack marbles and calculated C-O-H-F fluid compositions. American Mineralogist, 67, 545-557.

Van Orman, J.A., Grove, T.L., and Shimizu, N. (2001) Rare earth element diffusion in diopside: Influence of temperature, pressure, and ionic radius, and an elastic model for diffusion in silicates. Contributions to Mineralogy and Petrology, 141, 687-703.

661 Vanko, D.A. (1986) High-chlorine amphiboles from oceanic rocks: product of
662 highly-saline hydrothermal fluids? American Mineralogist, 71, 51-59.
663 Wallace, P.J. (2001) Volcanic SO2 emissions and the abundance and distribution of
664 exsolved gas in magma bodies. Journal of Volcanology and Geothermal
665 Research, 101, 85-106.
666 Wallace, P.J. (2005) Volatiles in subduction zone magmas: concentrations and fluxes
667 based on melt inclusion and volcanic gas data. Journal of Volcanology and
668 Geothermal Research, 140, 217-240.
669 Webster, J.D. (2004) The exsolution of magmatic hydrosaline chloride liquids.
670 Chemical Geology, 210, 33-48.
671 Webster, J.D., and Holloway, R. (1990) Partitioning of F and Cl between magmatic
672 hydrothermal fluids and highly evolved granite magmas. In Ore-bearing Granite
673 Systems; Petrogenesisa nd Mineralizing Processes (eds. H. J. Stein and J. C.
674 Hannah); GSA Special Paper 246. pp. 21-34.
675 Welch, M.D., Cámara, F., Ventura, G.D., and Iezzi, G. (2007) Non-Ambient in situ
676 Studies of Amphiboles. Reviews in Mineralogy and Geochemistry, 67, 223-260.
677 Wones, D.R., and Gilbert, M.C. (1982) Amphiboles in the igneous environment.
678 Reviews in Mineralogy and Geochemistry, 9B, 355-390.
679 Wood, S. A., and Normand, C. (2008) Mobility of palladium chloride complexes in
680 mafic rocks: insights from a flow-through experiment at 25 degrees C using
681 air-saturated, acidic, and Cl-rich solutions, Mineralogy and Petrology, 92,
682 81-97.

683 Xiao, Y.L., Hoefs, J., and Kronz, A. (2005) Compositionally zoned Cl-rich
684 amphiboles from North Dabie Shan, China. Monitor of high-pressure
685 metamorphic fluid/rock interaction processes. Lithos, 81, 279-295.
686 Zellmer, G.F., Blake, S., Vance, D., Hawkesworth, C., and Turner, S. (1999)
687 Plagioclase residence times at two island arc volcanoes (Kameni Islands,
688 Santorini,, Soufriere, St. Vincent) determined by Sr diffusion systematics.
689 Contributions to Mineralogy and Petrology, 136, 345-357.
690 Zhang, X.Y., Cherniak, D.J., and Watson, E.B. (2006) Oxygen diffusion in titanite:
691 lattice diffusion and fast-path diffusion in single crystals. Chemical Geology,
692 235, 105-123.
693 Zhang, Y. (2010) Diffusion in Minerals and Melts: Theoretical Background. Reviews
694 in Mineralogy and Geochemistry, 72, 5-59.
695 Zheng, Y. F., Fu, B., Gong, B., and Li, L. (2003) Stable isotope geochemistry of
696 ultrahigh pressure metamorphic rocks from the Dabie–Sulu orogen in China:
697 implications for geodynamics and fluid regime. Earth Science Review, 62,
698 105-161.
699 Zhu, C., and Sverjensky, D. (1991) Partitioning of F-Cl-OH between minerals and
700 hydrothermal fluids. Geochimica et Cosmochimica Acta, 55, 1837-1858.
701
702
703
704

705 FIGURE LEGENDS

706 Figure 1. Photographs of the marble sample from the Yunnan province, China. (a)
707 The marble contains very coarse homogeneous crystals of amphibole, clinopyroxene,
708 orthopyroxene, and epidote. The fine-grained matrix mainly consists of calcite +
709 dolomite. Hand specimen. (b-d) Micro-photographs reveal that the mineral
710 assemblage consists of clinopyroxene, orthopyroxene, epidote (b), calcite, dolomite
711 (c), and plagioclase, biotite, titanite and ilmenite (d). (e) Secondary electron image of
712 starting amphibole. It shows no compositional zonation. The spots in the figure are
713 analysis spots of the analytical traverse. Amphibole: Amp; clinopyroxene: Cpx;
714 orthopyroxene Opx; epidote: Epi; calcite:Cc; dolomite: Dol; plagioclase: Pl; biotite:
715 Bt; titanite: Ti; and ilmenite: Ilm.

716 Figure 2. Images of backscattered electron imaging and X-ray mapping of Cl, Fe,
717 Mg of amphibole of water-bearing experimental runs performed at 1.0 GPa, 750 °C
718 and 200 hours.

719 Figure 3. Measured chlorine diffusion profiles in water-bearing experiments. a:
720 Run number JL10, T = 625 °C, P = 1.0 GPa, t = 454 h; b: Run number JL1, T =
721 650 °C, P = 1.0 GPa, t = 100 h; c: Run number JL5 T = 700 °C, P = 1.0 GPa, t = 200 h;
722 d: Run number JL3, T = 750 °C, P = 1.0 GPa, t = 200 h; e: Run number JL7, T =
723 800 °C, P = 1.0 GPa, t = 100 h. The smooth curve is the best fit of the EMPA data
724 with a diffusion model.

725 Figure 4. Traverse of $^{37}Cl/^{30}Si$ in amphibole of experiment number JL3 (T =
726 750 °C, P = 1.0 GPa, t = 200 h). The smooth curve is the best fit of the SIMS data

727 with a diffusion model. a: micro-image of sputtered crater within the sample by FIB;
728 b: Traverse profile of $^{37}Cl/^{30}Si$.

729 Figure 5. Arrhenius plot of Chlorine (Cl) diffusion in amphibole of runs
730 performed at 1.0 GPa, from 625 °C to 800 °C.

731 Figure 6. Arrhenius plot summarizing diffusion studies in amphiboles. Hydrogen
732 data from Ingrin et al. (2000) [H(1)], Graham et al. (1984) [H(2), H(3)], respectively.
733 F-OH data from Brabander et al. (1995). Oxygen data from Farver and Giletti (1985).
734 Ar data from Harrison (1981). Sr data from Brabander and Giletti (1995). Chlorine
735 (Cl) data are from this study.

736 Figure 7. Plots of Cl, F and other elements in amphibole from water-bearing
737 experimental runs performed at 1.0 GPa, from 625 °C to 800 °C, respectively. a: Cl vs
738 F; b: Cl vs FeO; c: Cl vs MgO; d: F vs FeO; e: F vs MgO.

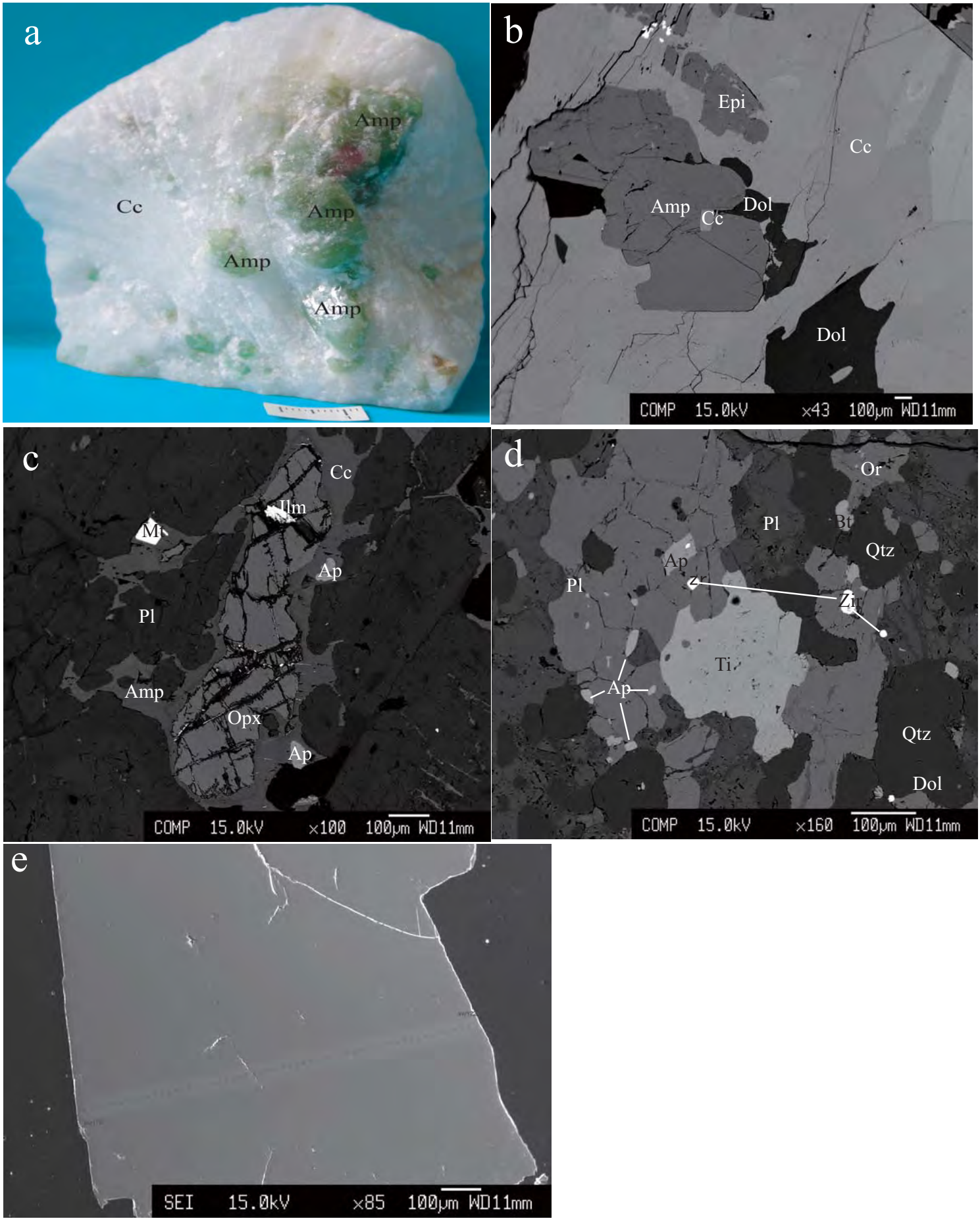
a
Amp
Cc
Amp
Amp
Amp
b
Epi
Cc
Amp
Cc
Dol
Dol
COMP 15.0kV ×43 100µm WD11mm
c
Cc
Ilm
Mt
Ap
Pl
Amp
Opx
Ap
COMP 15.0kV ×100 100µm WD11mm
d
Or
Pl
Bt
Qtz
Ap
Pl
Zr
Ti
Ap
Qtz
Dol
COMP 15.0kV ×160 100µm WD11mm
e
SEI 15.0kV ×85 100µm WD11mm

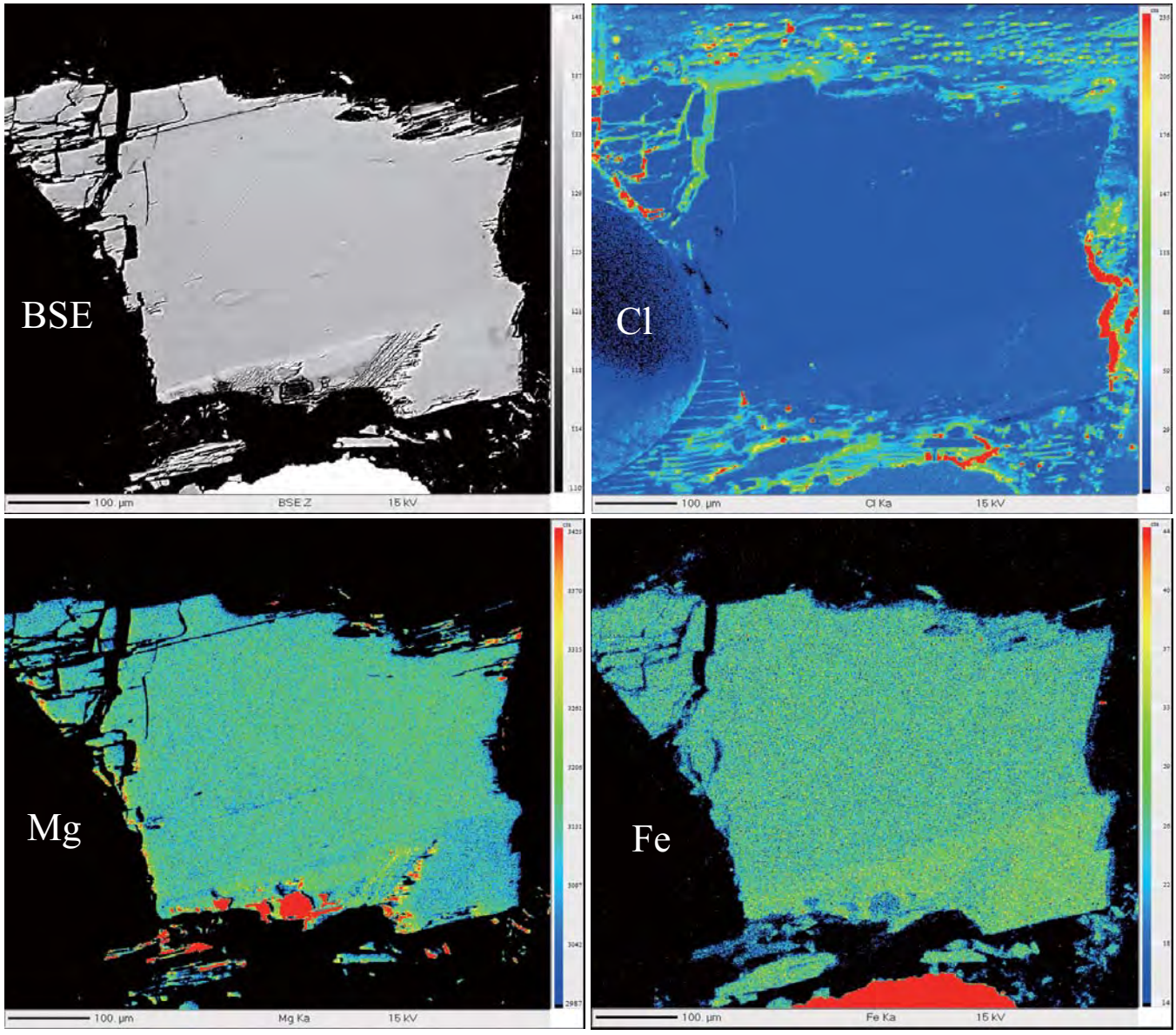
BSE
100. µm
BSE Z
15 kV
Cl
100. µm
Cl Ka
15 kV
Mg
100. µm
Mg Ka
15 kV
Fe
100. µm
Fe Ka
15 kV

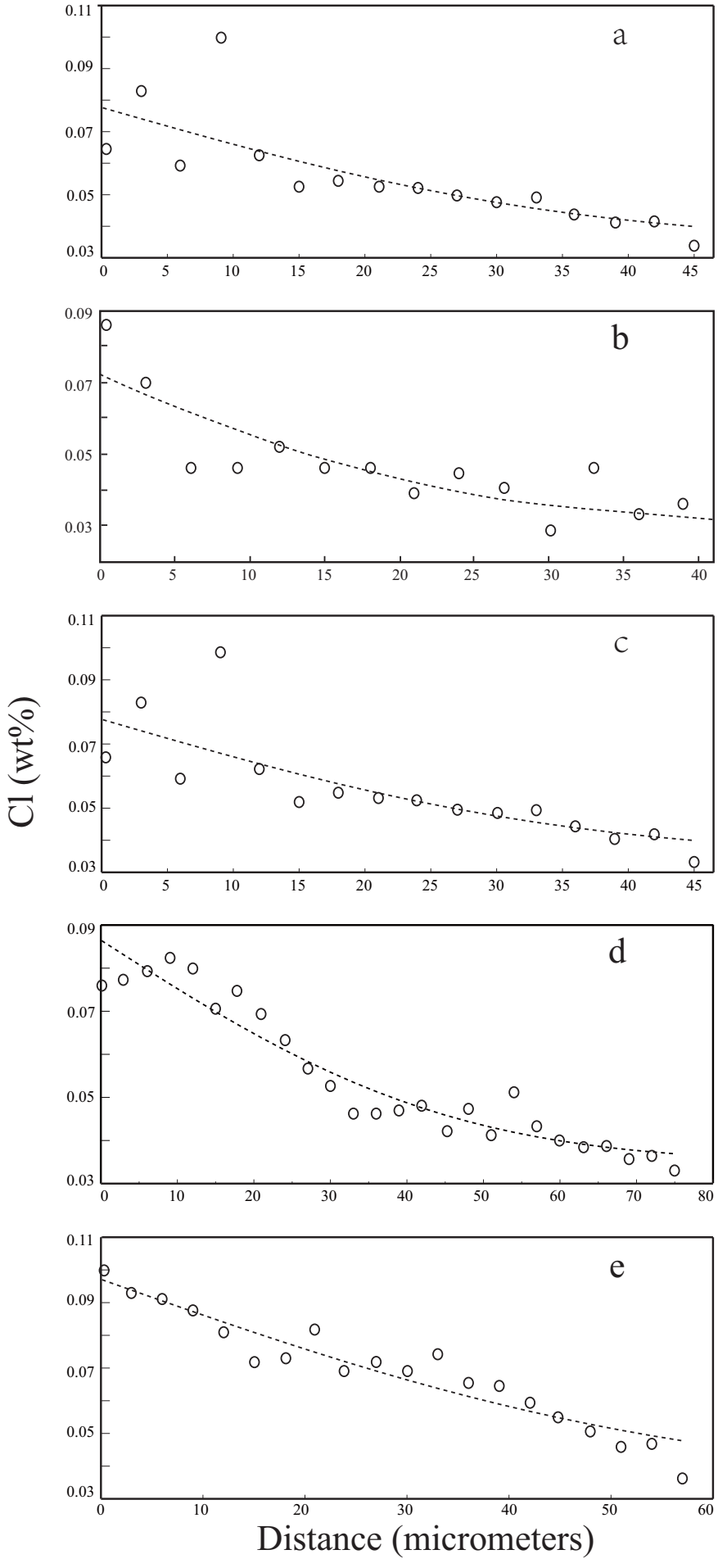
a
b
c
d
e
Cl (wt%)
Distance (micrometers)

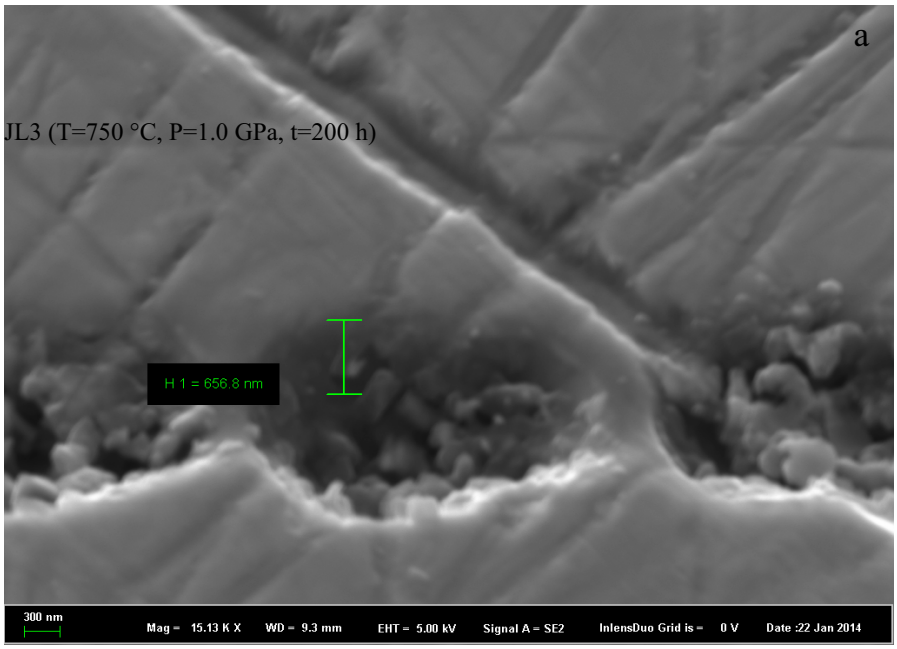
a
JL3 (T=750 °C, P=1.0 GPa, t=200 h)
H 1 = 656.8 nm
300 nm
Mag = 15.13 K X
WD = 9.3 mm
EHT = 5.00 kV
Signal A = SE2
InlensDuo Grid is = 0 V
Date :22 Jan 2014

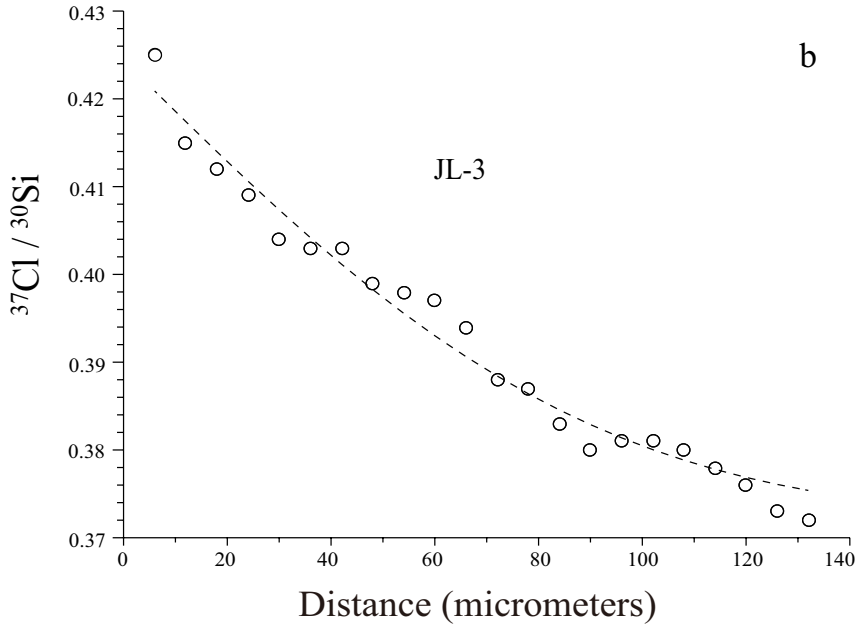
b
JL-3
^{37}Cl / ^{30}Si
0.43
0.42
0.41
0.40
0.39
0.38
0.37
0
20
40
60
80
100
120
140
Distance (micrometers)

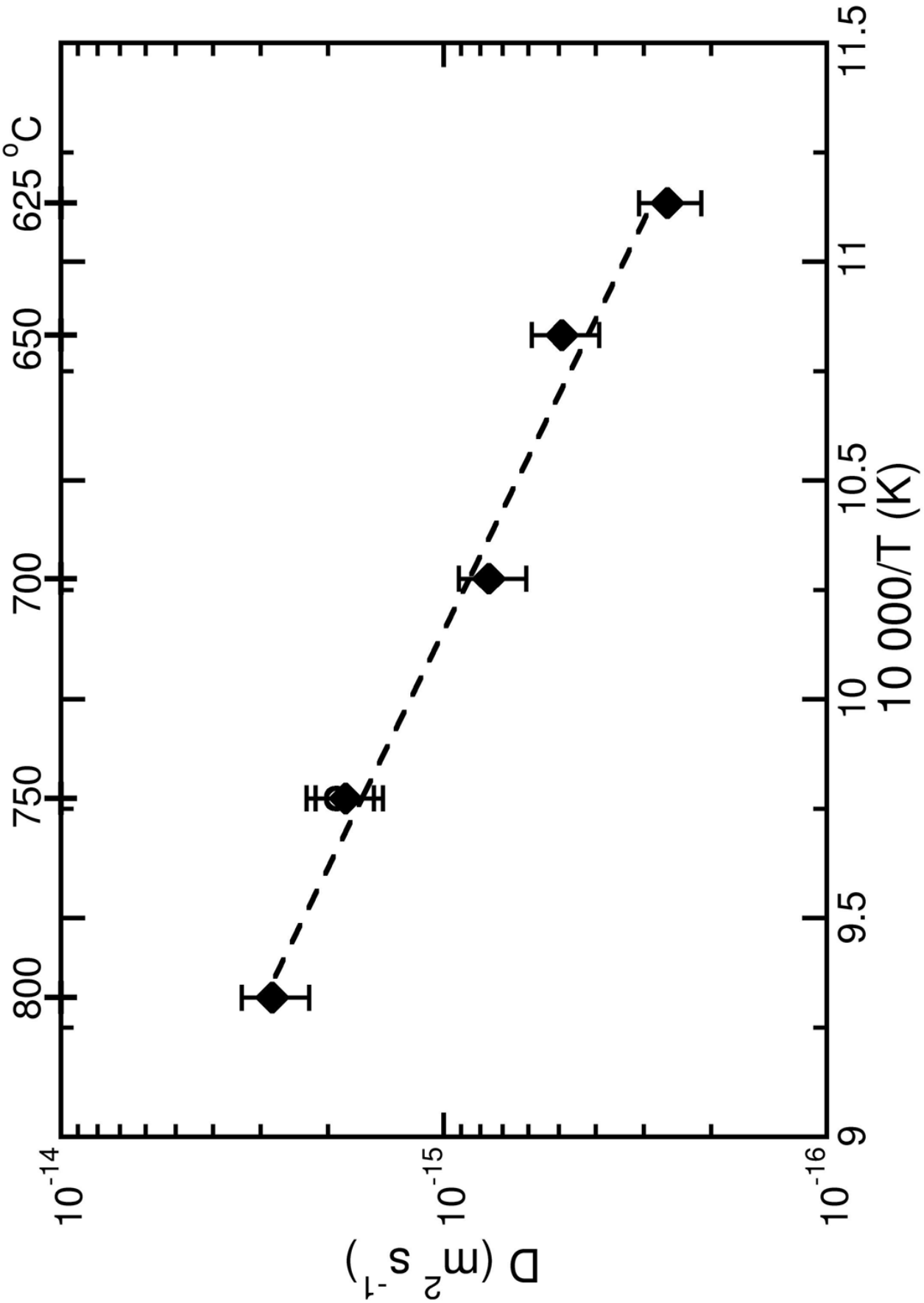
625 °C
650
700
750
800
11.5
11
10.5
10
9.5
9
10 000/T (K)
10^-14
10^-15
10^-16
D (m^2 s^-1)

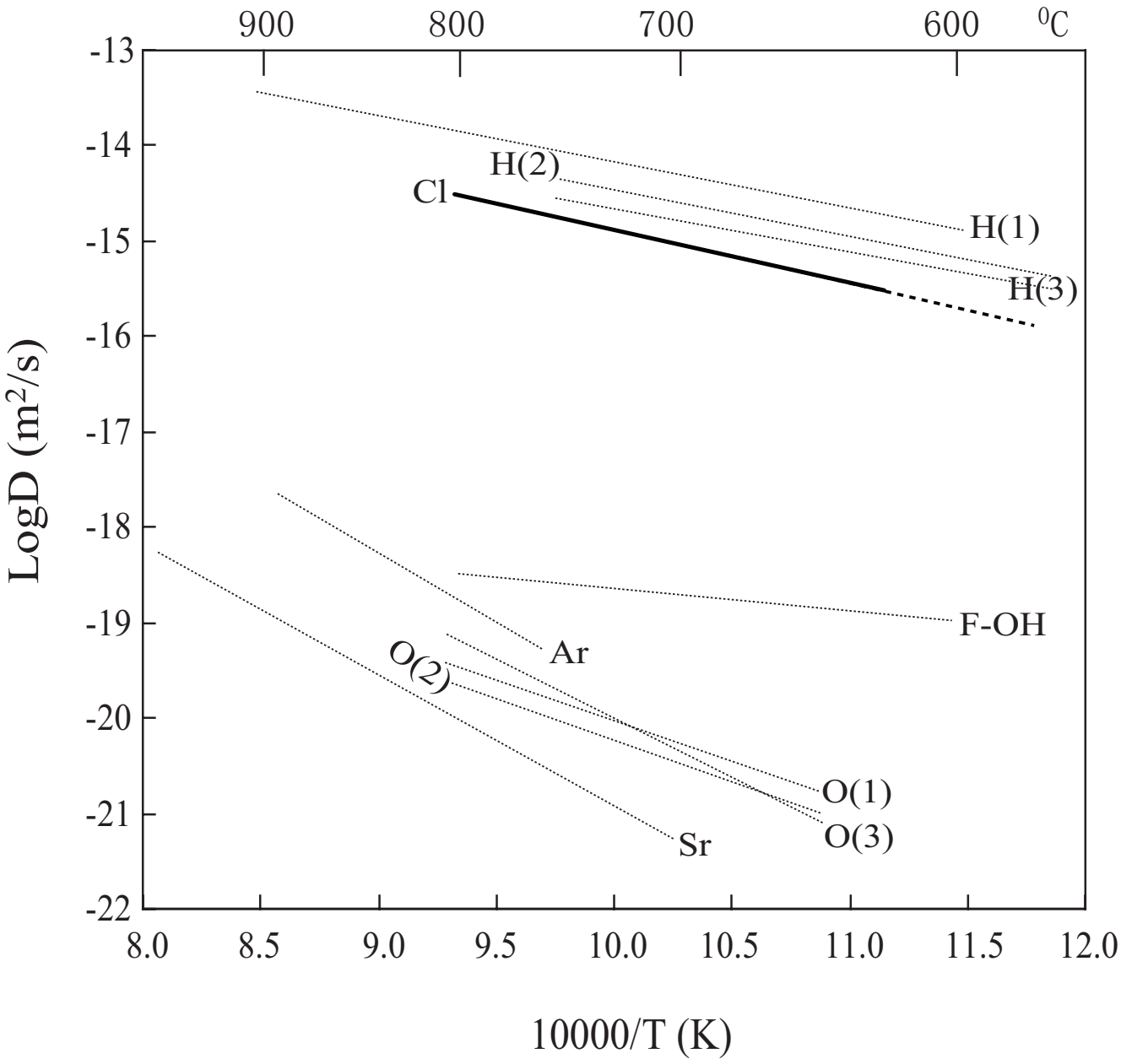
900
800
700
600
^{0}C
-13
-14
-15
-16
-17
-18
-19
-20
-21
-22
LogD (m^2/s)
H(2)
Cl
H(1)
H(3)
Ar
F-OH
O(2)
O(1)
O(3)
Sr
8.0
8.5
9.0
9.5
10.0
10.5
11.0
11.5
12.0
10000/T (K)

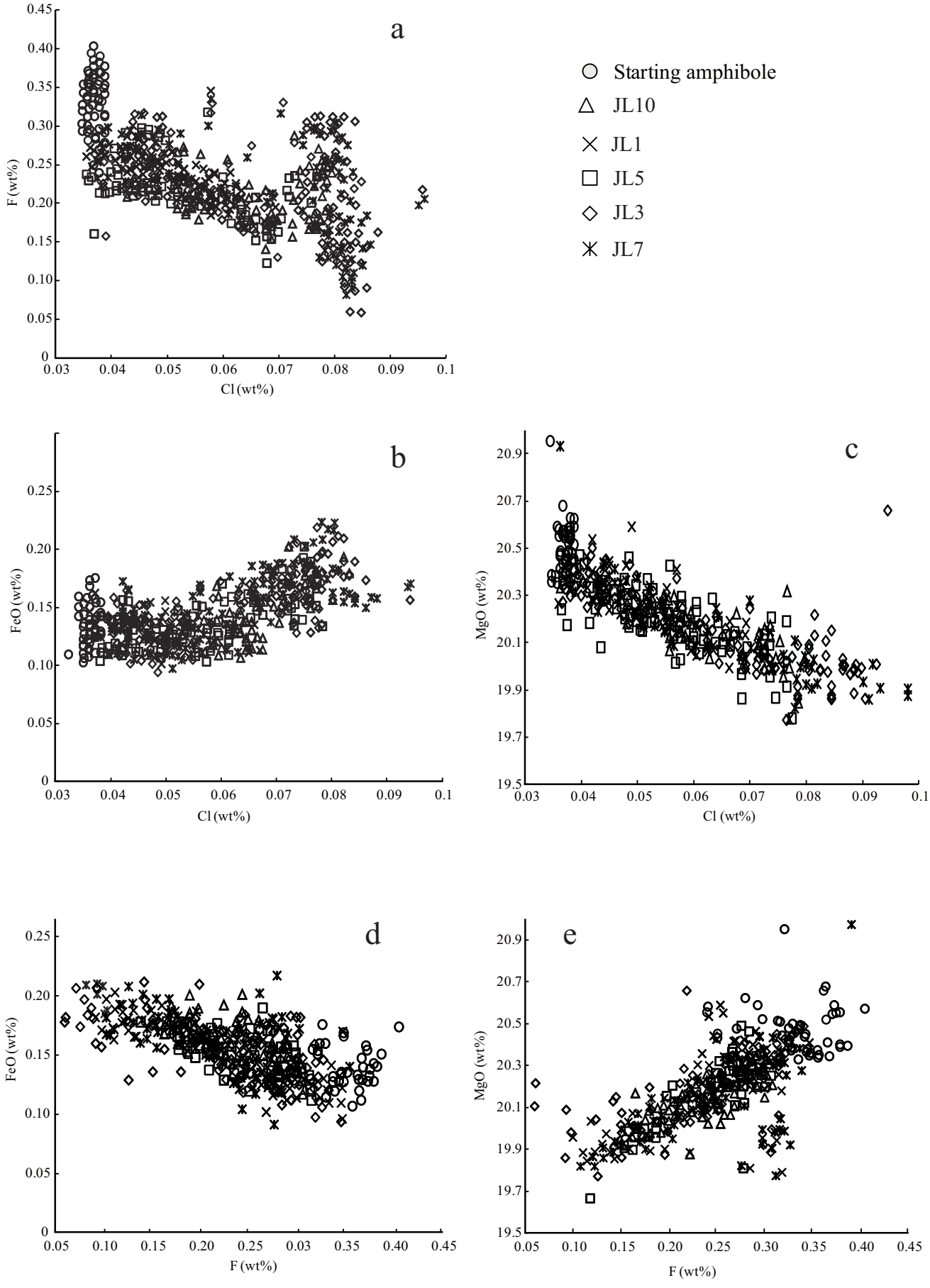
a
F (wt%)
Cl (wt%)
Starting amphibole
JL10
JL1
JL5
JL3
JL7
b
FeO (wt%)
Cl (wt%)
c
MgO (wt%)
Cl (wt%)
d
FeO (wt%)
F (wt%)
e
MgO (wt%)
F (wt%)

Table 1. Electron microprobe analyses of starting amphiboles and its paragenous minerals from the marble (sample No. JL) (wt %)

Mineral/Spots	SiO2	TiO2	Cr2O3	Al2O3	FeO	MgO	MnO	CaO	Na2O	K2O	Cl	F	Total
Amphibole	44.30	0.54	0.09	14.18	0.14	20.52	0.00	13.38	2.38	0.20	0.031	0.34	96.11
Line1	44.68	0.53	0.08	14.35	0.13	20.52	0.00	13.31	2.43	0.21	0.032	0.33	96.58
Line2	44.30	0.53	0.07	14.54	0.14	20.48	0.00	13.23	2.41	0.22	0.033	0.35	96.29
Line3	44.17	0.58	0.05	14.45	0.17	20.36	0.01	13.33	2.40	0.21	0.030	0.35	96.11
Line4	44.40	0.56	0.08	14.39	0.15	20.50	0.00	13.44	2.43	0.21	0.033	0.36	96.55
Line5	44.23	0.60	0.05	14.53	0.13	20.45	0.00	13.39	2.39	0.23	0.033	0.34	96.37
Line6	44.14	0.55	0.11	14.46	0.11	20.67	0.01	13.27	2.38	0.22	0.031	0.33	96.27
Line7	44.06	0.57	0.05	14.32	0.16	20.55	0.00	13.32	2.42	0.22	0.031	0.37	96.07
Line8	44.25	0.57	0.08	14.33	0.10	20.62	0.00	13.37	2.41	0.23	0.033	0.37	96.36
Line9	44.36	0.58	0.03	14.22	0.13	20.59	0.00	13.31	2.41	0.22	0.030	0.37	96.24
Line10	44.21	0.56	0.05	14.37	0.12	20.68	0.01	13.32	2.41	0.21	0.030	0.36	96.33
Line11	44.29	0.55	0.06	14.24	0.14	20.40	0.02	13.45	2.39	0.23	0.032	0.38	96.18
Line12	44.24	0.55	0.05	14.26	0.18	20.43	0.01	13.38	2.41	0.21	0.031	0.33	96.06
Line13	44.35	0.56	0.04	14.36	0.13	20.56	0.00	13.34	2.47	0.22	0.030	0.38	96.43
Line14	43.96	0.56	0.07	14.75	0.14	20.35	0.00	13.43	2.43	0.22	0.030	0.37	96.28
Line15	44.40	0.61	0.10	14.24	0.15	20.59	0.01	13.39	2.40	0.22	0.032	0.34	96.49
Clinopyroxene	53.31	0.18	0.05	0.74	7.20	14.55	0.25	22.49	0.20	0.03	0.00	un	99.00
Orthopyroxene	54.36	0.09	0.01	0.62	20.51	23.35	0.63	0.84	0.05	0.00	0.01	un	100.47
Epidote	38.44	0.06	0.01	28.80	5.20	0.04	0.08	23.51	0.01	0.01	0.00	un	96.16
Plagioclase	56.03	0.07	0.00	28.18	0.29	0.03	0.00	10.70	5.20	0.24	0.00	un	100.74
Biotite	35.48	4.76	0.02	13.15	21.98	9.65	0.14	0.05	0.16	8.57	0.15	un	94.11
Ilmenite	0.02	50.52	0.05	0.02	46.19	0.04	2.49	0.25	0.01	0.00	0.01	un	99.60
Titanite	30.78	36.73	0.08	1.88	0.68	0.03	0.00	28.60	0.04	0.02	0.01	un	98.85
Dolomite	0.00	0.00	0.00	0.00	0.06	19.52	0.05	30.50	0.01	0.00	0.00	un	50.14
Calcite	0.00	0.00	0.03	0.03	0.04	1.45	0.00	52.78	0.01	0.01	0.00	un	54.35

un—unanalysis.

Table 2. Experimental conditions and diffusion coefficients for chlorine at 1.0 GPa in the amphibole

Run No.	T ( )	P (GPa)	Time (h)	H_2O(ug)	No. traverses/ error	D(m^2/s)	Analysis method
JL10	625	1.0	454	Add(0.23)	6/20%	2.6×10^{-16}	EMPA
JL1	650	1.0	100	Add(0.49)	8/18%	4.9×10^{-16}	EMPA
JL5	700	1.0	200	Add(1.36)	8/16%	7.6×10^{-16}	EMPA
JL3	750	1.0	200	Add(3.29)	8/16%	1.8×10^{-15}	EMPA
JL3	750	1.0	200	Add(3.29)	1	1.9×10^{-15}	SIMS
JL7	800	1.0	100	Add(3.81)	4/16%	2.8×10^{-15}	EMPA

Table 3. Summarize best fit parameters to the Arrhenius equations for elements diffusion in the amphiboles

Element	T (℃)	P (GPa)	$D_0(m^2/s)$	Ea(kJ/K mol)	Reference
hydrogen	350 - 800	0.2-0.8		79-84(Hb) 71.5(Tr) 99(Act)	Graham et al. (1984)
hydrogen	600 - 900	0.01		104 ± 12(Kat)	Ingrin and Blanchard (2000)
oxygen	650 - 800	0.1		172 ± 25(Hb) 163 ± 21(Tr) 238 ± 8(F-Rict)	Farver and Giletti (1985)
F-OH	500 - 800	0.2	3.4×10^{-17}	41 ± 5	Brabander et al. (1995)
Sr			4.9×10^{-8}	260 ± 12(Hb)	Brabander and Giletti (1995)
Ar					Harrison (1981)
Ar					Baldwin et al. (1990)
Cl	625-800	1.0	$4.53(+7.3, -2.8) \times 10^{-10}$	106.6 ± 7.8	This study